

## Vortex-liquid–vortex-crystal transition in type-II superconductors

T. J. Newman\*

*Institut für Theoretische Physik, Universität zu Köln, D-50937 Köln, Germany  
and Theoretical Physics, University of Oxford, Oxford, OX1 3NP, United Kingdom*

M. A. Moore

*Department of Physics, University of Manchester, Manchester, M13 9PL, United Kingdom*

(Received 27 November 1995; revised manuscript received 11 March 1996)

We present in detail a functional renormalization group (FRG) study of a Landau-Ginzburg model of type-II superconductors (generalized to  $N/2$  complex fields) in an external magnetic field, both for a pure system and also in the presence of quenched random impurities. If the coupling functions are restricted to the space of functions with nonzero support only at reciprocal lattice vectors corresponding to the Abrikosov lattice, we find a stable FRG fixed point in the presence of disorder for  $1 < N < 4$ , identical to that of the disordered  $O(N)$  model in  $d-2$  dimensions. This implies a continuous transition from the vortex crystal to vortex liquid in the presence of disorder, but only for  $d > 4$ . The nonzero-temperature transition will disappear in physical dimensions. The pure system has a stable fixed point only for  $N > 4$ . Therefore the physical case ( $N=2$ ) is likely to have a first-order transition in the absence of quenched disorder. We give a full discussion of both the motivation of the model and the details of the FRG calculation. We also place our results in context with regard to the current experimental scene concerning the high- $T_c$  compounds. In particular, we discuss the relevance of our results to the recently discovered critical end point in the phase diagram of Bi-Sr-Ca-Cu-O. The main results of this analysis were previously reported in the form of a Letter [M.A. Moore and T.J. Newman, Phys. Rev. Lett. **75**, 533 (1995)]. [S0163-1829(96)01833-4]

### I. INTRODUCTION

With the advent of the new high- $T_c$  materials, there has been a regeneration of interest in the nature of the “mixed phase” in type-II superconductors. In conventional materials, the effect of fluctuations is severely reduced due to both the large coherence length and the relatively low temperatures. The phase diagram is therefore quite simple: The Meissner and normal phases are separated by a vortex crystal phase in which the magnetic flux penetrates the sample in the form of a triangular array — the Abrikosov lattice.<sup>1</sup> In high- $T_c$  compounds, the much smaller coherence length, together with the moderately high temperatures, allows fluctuations to act much more strongly. This gives rise to the possibility of a richer phase diagram. Interesting complications are also induced by both the effects of disorder and of the strongly layered structure of the new compounds.

The phenomenological approach to understanding the phase diagram of the high- $T_c$  compounds centers on the Landau-Ginzburg free energy, which is written in terms of two fields: the superconducting order parameter  $\psi$  and the vector potential  $\mathbf{A}$ . Most theoretical efforts have been within one of two complimentary approaches, namely, the London picture and the lowest-Landau-level (LLL) approximation. The London picture focuses directly on the vortex lines, ignoring fluctuations of the amplitude of the order parameter. This appears to be an adequate description for low fields, where the vortex core is much smaller than the typical inter-vortex separation, and the amplitude of the order parameter may then be taken as approximately constant over most of the system. Conversely, the LLL approach ignores fluctuations in the vector potential and concentrates solely on order

parameter fluctuations. Furthermore, it is assumed that all Landau levels except the lowest will *smoothly renormalize* the physics, thereby allowing one to work solely within the LLL. This approach is well suited for the high-field regime in strongly type-II superconductors, where the ratio  $\kappa$  of the London penetration depth to the coherence length is large. Whether these two approaches overlap in their regimes of validity appears to be an open question.

In this current work we wish to concentrate on the transition from the vortex liquid to the vortex crystal, which is the fluctuation-corrected analog of the Abrikosov mean-field transition from the normal metal to the Abrikosov flux lattice, usually denoted by  $H_{c2}(T)$ . We shall work solely within the LLL scheme. The two basic questions we wish to answer are the following: (i) In the pure system, what is the nature of the phase transition between vortex liquid and vortex crystal, and (ii) how is this transition affected by the presence of quenched random impurities? To address the first question one must extend the original mean-field analysis of Abrikosov to take into account thermal fluctuations of the order parameter. This was first attempted by Brézin, Nelson, and Thiaville (BNT) in 1985, using a functional renormalization group (FRG) method.<sup>2</sup> It was found in the early stages of the present work that their representation of the FRG was not always sensitive to the existence of a FRG fixed point (which registers a possible continuous phase transition), and therefore the question of the role of fluctuations was still open. We use here a more sensitive representation of the FRG.

Our main conclusion is, however, the same as that of BNT — no stable fixed point of the FRG exists, thereby indicating that the vortex liquid to vortex crystal (VLVC) transition for the pure system is probably first order. The

second question regarding the role of disorder may be addressed by using similar FRG techniques. It is well known that quenched disorder can often force a first-order transition into a continuous one.<sup>3</sup> An interesting example of this is the transition from the normal metal to the Meissner phase which, although first-order for a pure sample,<sup>4</sup> is driven to a continuous transition in the presence of disorder.<sup>5</sup> Indeed, in the current problem, we find that disorder dramatically changes the FRG flow, and there exists a stable FRG fixed point in this case, indicating that disorder can force the otherwise first-order transition into a continuous one. However, we have arguments which show that this continuous transition has a lower critical dimension of 4, which implies that the physical superconductor (existing in  $d=3$ ) undergoes no VLVC transition in the presence of weak disorder. The main results of this work were presented in a recent Letter.<sup>6</sup>

The purpose of this paper is first to give a detailed derivation of the results and second to discuss the relevance of the results in the context of the present theoretical and experimental scene.

The outline of the paper is as follows. In the next section we shall present the Landau-Ginzburg free energy functional and discuss the simplifications which may be made under the LLL approximation. Our treatment shall closely follow that of BNT, but we include such a discussion here purely for completeness. In Sec. III, we shall outline the procedure of the FRG method. Again, we shall be following the presentation of BNT somewhat, although we shall find it necessary to avoid their representation of the FRG for reasons mentioned above. We shall present a representation which is more sensitive to the existence of fixed points, and derive in some detail the FRG flow equations for both the pure system and the disordered system.

The next two sections may be omitted by the reader who is mostly interested in the main results. In Sec. IV we present our attempts to analytically derive the solution of the flow equations. The special limits in which some progress is possible are the limits  $N \rightarrow \infty$  and  $N=0$ . (The variable  $N$  is often used to allow the possibility of such solvable limits. It is introduced by extending the complex order parameter  $\psi$  to a set of  $N/2$  complex fields  $\psi_i$ .) In the former case, we shall make contact with recent calculations devoted to the large- $N$  limit of this model for arbitrary dimensions.<sup>7,8</sup> The corrections to the large- $N$  limit will be shown here to be ill defined in the thermodynamic limit, which we interpret as a precursor of the VLVC transition. For the limiting case of  $N=0$  we shall see that the small- $N$  corrections are nonanalytic. A scaling approach is required to correctly extract the small- $N$  behavior. The resulting flow equation for the scaling function has a beautiful structure which we consider worthy of study in its own right. The superconductor corresponds to  $N=2$  and is beyond brute force analytic treatment. In Sec. V, we shall briefly discuss our (failed) attempts at numerically solving the flow equations for this case. Both discrete ‘‘time’’ iteration and Newton root-finding schemes shall be discussed.

The flow equations are made analytically tractable by the application of a physical idea: Since the ordered state is that of a vortex crystal, the fixed point of the model should have some symmetry associated with this lattice structure. In Sec. VI, we motivate and present the reciprocal lattice vector

(RLV) *Ansatz* for the fixed point. The implications of this *Ansatz* are discussed in Sec. VII, in which we present the fixed point structure of the FRG flow (along with associated critical exponents) for both the pure and disordered systems within this RLV scheme. We end the paper with Sec. VIII, which is devoted to a detailed discussion of our results in the context of recent experiments and current theoretical understanding.

## II. LANDAU-GINZBURG FREE ENERGY

In this section we shall motivate the LLL approximation for the free energy, starting from the Landau-Ginzburg formulation of superconductors. For simplicity we shall mostly discuss the case of no disorder. Our presentation closely follows that of BNT, and the inclusion of such a detailed description here is for the sake of completeness.

The starting point of the analysis is the Landau-Ginzburg free energy functional for type-II superconductors (in standard notation,<sup>9</sup> with the additional convention of setting  $\hbar = c = k_B = 1$ ):

$$F = \int d^d r \left[ \frac{1}{2m^*} |(\nabla + ie^* \mathbf{A}) \psi_i|^2 + a |\psi_i|^2 + b |\psi_i|^2 |\psi_j|^2 + \frac{1}{2\mu_0} (\nabla \times \mathbf{A} - \mathbf{H})^2 \right], \quad (1)$$

where  $\{\psi_i\}$  are a set of  $N/2$  complex order parameters (the implicitly repeated indices  $i$  and  $j$  are to be summed from 1 to  $N/2$ ),  $\mathbf{A}$  is the vector potential, and  $\mathbf{H}$  is the external magnetic field. We have written the theory for arbitrary spatial dimensionality  $d$ . In the physical case of  $d=3$ , the external field  $\mathbf{H} \parallel \hat{z}$  picks out a transverse plane ( $x, y$ ) in which the Abrikosov lattice is formed. In general  $d$ , we define the field  $\mathbf{H}$  to be directed in a  $d-2$  hyperplane  $\mathbf{r}_\perp$ , so that the Abrikosov lattice is still confined to the two-dimensional ( $x, y$ ) plane transverse to this field.

We wish to work in the LLL approximation. First, we assume that we may neglect fluctuations in the vector potential. We believe this to be a good approximation for high external fields and for materials in which the ratio of the London penetration depth  $\lambda$  to the coherence length  $\xi$  is large. In this case, the magnetic field will fluctuate only over distances large compared with the intervortex separation, and we therefore consider it as uniform. It is worth mentioning that within the context of the renormalization group, the existence of stable fixed points allows one to discuss the relevance of new operators in the theory. We refer the reader to BNT, where it is explicitly demonstrated that gauge field fluctuations are *irrelevant* operators if a fixed point exists within the LLL scheme. By choosing the ‘‘symmetric’’ gauge,  $\mathbf{A}_0 = H/2(-y, x; \mathbf{0})$ , we reduce the free energy to the form

$$F = \int d^d r \left[ \frac{1}{2m^*} |(\nabla + ie^* \mathbf{A}_0) \psi_i|^2 + a |\psi_i|^2 + b |\psi_i|^2 |\psi_j|^2 \right]. \quad (2)$$

Now that the magnetic field is taken as spatially uniform it is convenient to expand the order parameter in terms of Landau levels. These are the eigenfunctions of the operator

$$h_0 = \frac{1}{2m^*} (i\nabla + e^* \mathbf{A}_0)^2 \quad (3)$$

and are simple harmonic oscillator wave functions  $U_{n,m}(x,y)$  [with associated energy eigenvalues  $E_n = (n+1/2)e^*H/m^*$ ]. The index  $n$  labels the energy eigenvalue, while  $m$  labels the degeneracy [which is proportional to the system size in the  $(x,y)$  plane]. One may now diagonalize the quadratic terms in the free energy by expanding the order parameter in the Landau level basis

$$\psi_i(x,y;\mathbf{r}_\perp) = \sum_{n,m} c_{n,m}^i(\mathbf{r}_\perp) U_{n,m}(x,y). \quad (4)$$

The quadratic part of the free energy now takes the form

$$F_{\text{quad}} = \sum_{n,m} \int d^{d-2}r_\perp \left[ \frac{1}{2m^*} |\nabla_\perp c_{n,m}^i|^2 + (a + E_n) |c_{n,m}^i|^2 \right]. \quad (5)$$

On reducing the size of the external field, the amplitude of the second term in the above expression first becomes zero for the mode  $c_{0,m}^i$  — this occurs for a value of the field equal to  $H_{c2}(T)$  defined by the relation  $E_0 = -a(T)$ . The higher Landau modes have positive coefficients at this value of the external field. If one is interested in the critical region, the higher Landau modes may therefore be neglected. [The validity of this statement relies on the shift in  $H_{c2}$  caused by inclusion of the quartic (fluctuation) terms not being greater than the bare separation of the Landau modes (which is proportional to  $H$ ). This ‘‘Ginzburg criterion’’-type analysis has been studied in detail<sup>10</sup> with the conclusion that exclusion of all Landau modes except the lowest is a valid procedure for a wide range of fields below the mean-field value  $H_{c2}$ .] Naturally, these ideas are applicable under the *a priori* assumption of a continuous transition.

On restricting ones attention to the LLL, a great simplification may be made to the form of the free energy, which will set the stage for all the FRG analysis to follow. In the symmetric gauge, the  $n=0$  Landau levels may be represented by the eigenfunctions ( $m>0$ )

$$U_{0,m} = A_m (x+iy)^m \exp[-\mu^2(x^2+y^2)/4], \quad (6)$$

where  $A_m$  is a normalization constant and  $\mu^2 \equiv e^*H$ . Since  $\psi_i$  is now taken to be expressed only in terms of these LLL modes, we see that the order parameter in the critical region is simply an arbitrary function of  $z=x+iy$  along with an overall factor of  $\exp[-\mu^2(x^2+y^2)/4]$ . Explicitly, we have

$$\psi_i(x,y;\mathbf{r}_\perp) = \phi_i(z,\mathbf{r}_\perp) \exp(-\mu^2 z^* z/4), \quad (7)$$

where  $\phi_i$  is holomorphic in terms of  $z$  (i.e.,  $\partial\phi_i/\partial z^* = 0$ ).

In terms of the new order parameter  $\phi_i$  (suitably scaled) we have the following elegant form of the free energy in the critical region:

$$F = \int d^{d-2}r \int dz dz^* [ (|\nabla_\perp \phi_i|^2 + \tau |\phi_i|^2) \exp(-\mu^2 z^* z/2) + g_0 |\phi_i|^2 |\phi_j|^2 \exp(-\mu^2 z^* z) ], \quad (8)$$

where the parameter  $\tau = 2m^*a(T) + e^*H$  is proportional to  $H - H_{c2}$ .

We now address the inclusion of quenched random impurities into the above formalism. We regard the disorder to have the physical effect of inducing a local shift to the critical temperature. Therefore the original Landau-Ginzburg free energy is modified by replacing the parameter  $a$  by  $[a + \delta a(\mathbf{r})]$ . The random field  $\delta a(\mathbf{r})$  is taken to be Gaussian distributed with zero mean and correlator  $\langle \delta a(\mathbf{r}) \delta a(\mathbf{r}') \rangle = \Delta_0 \delta^d(\mathbf{r} - \mathbf{r}')$ . We shall regard the disorder to be weak, such that  $\Delta_0 \ll 1$ . The standard ways to deal with such a disorder term are twofold. Since one is eventually interested in some perturbative treatment of the free energy about the Gaussian theory (defined by  $F_{\text{quad}}$ ), one may regard the term  $\delta a(\mathbf{r}) |\psi_i(\mathbf{r})|^2$  as a second coupling term in addition to the usual quartic interaction. One then perturbs in both interactions and averages the perturbation expansions over the distribution of  $\delta a(\mathbf{r})$ . The effect of such averaging is to highlight the fact that the disorder may in fact be interpreted as an effective *quartic* interaction<sup>11</sup> with strength  $(-\Delta_0)$ . An alternative (yet mathematically identical) procedure is to average over the disorder at the level of the partition function. Since the disorder is quenched, one must average the logarithm of the partition function (which is extensive) and this is most easily achieved with the use of replicas. The resulting free energy now contains the remains of the disorder in terms of an effective quartic interaction, again with strength  $(-\Delta_0)$ . For notational convenience we shall use the latter approach. We emphasize that the use of replicas here is purely to ‘‘keep track’’ of the disorder in perturbation theory.

The effective free energy now takes the form

$$F = \int d^d r \left[ \frac{1}{2m^*} |(\nabla + ie^* \mathbf{A}) \psi_i^\alpha|^2 + a |\psi_i^\alpha|^2 + b |\psi_i^\alpha|^2 |\psi_j^\alpha|^2 - \Delta_0 |\psi_i^\alpha|^2 |\psi_j^\beta|^2 + \frac{1}{2\mu_0} (\nabla \times \mathbf{A} - \mathbf{H})^2 \right], \quad (9)$$

where the order parameter has an extra (replica) index  $\alpha$  which is to be implicitly summed from 1 to  $M$ . At the end of the calculation  $M$  is to be set to zero. Following all of the above steps as described for the pure system, we may use the LLL approximation to simplify the above free energy to the form

$$F = \int d^{d-2}r \int dz dz^* [ (|\nabla_\perp \phi_i^\alpha|^2 + \tau |\phi_i^\alpha|^2) \exp(-\mu^2 z^* z/2) + g_0 |\phi_i^\alpha|^2 |\phi_j^\alpha|^2 \exp(-\mu^2 z^* z) - \Delta_0 |\phi_i^\alpha|^2 |\phi_j^\beta|^2 \times \exp(-\mu^2 z^* z) ]. \quad (10)$$

This concludes our description of the model. In the next section we shall motivate the FRG by considering perturbation theory for the above free energy. We shall then describe, in some detail, the intricacies of the representation of the FRG. The goal of the next section is to derive the most natural FRG flow equations for this model.

### III. FUNCTIONAL RENORMALIZATION GROUP

For convenience we shall discuss the procedure of FRG within the pure model ( $\Delta_0=0$ ). The influence of the disorder

is easily accounted for once the correct FRG framework is established. In order to study the effect of fluctuations on the Abrikosov mean-field transition, we follow the standard procedure of setting up a perturbation expansion around the Gaussian theory in powers of the quartic coupling  $g_0$ . The terms in the expansion are most conveniently represented as Feynman diagrams with the two basic components being the propagator  $\sigma(\mathbf{q}_\perp; z_1^*, z_2)$  and the bare vertex. The propagator is the inverse of the quadratic form in the energy functional (8). As shown by BNT, the propagator takes the form [using a momentum representation for the  $d-2$  hyperplane transverse to the  $(x, y)$  plane]

$$\sigma(\mathbf{q}_\perp; z_1^*, z_2) = \frac{1}{(q_\perp^2 + \tau)} \frac{\mu^2}{2\pi} \exp(\mu^2 z_1^* z_2 / 2), \quad (11)$$

while the bare vertex is clearly given by  $-g_0 \exp(-\mu^2 z^* z)$ .

If one tries to simply calculate the one-loop terms in the perturbation expansion, one finds the transverse momentum integrals diverge when  $d-2 < 4$  (just as one would expect for a quartic theory, except here the momenta are defined in a reduced space of  $d-2$  dimensions). This condition sets the upper critical dimension  $d_u = 6$ . For  $d > d_u$  the perturbation expansion contains no divergences and the mean-field results will be qualitatively unchanged. However, for  $d < d_u$  the simple perturbation scheme breaks down. One way to proceed is to utilize the renormalization group. It is important to notice in the present theory that the renormalization group is required to ‘‘cure’’ the divergences that arise from critical fluctuations in the  $d-2$  transverse directions. The fluctuations in the  $(x, y)$  plane are not critical and the integrals over  $(z, z^*)$  may be regarded as (complicated) coefficients to the momentum integrals in the transverse directions. The fact that these coefficients are really functions (of  $z$  and  $z^*$ ) will eventually lead us to generalize the renormalization group to a functional form.

Let us imagine proceeding with a renormalization group calculation using the dimensional regularization technique.<sup>12</sup> The perturbation expansion of the free energy functional (8) may be considered as a loop expansion in powers of  $\epsilon \equiv 6 - d$ . On calculating the one-loop vertex corrections, one is faced with a severe problem (as described in detail by BNT). The bare vertex carries an overall factor of  $\exp(-\mu^2 z^* z)$ . The one-loop corrections must also carry this factor in order to consistently renormalize the bare vertex. However, this turns out not to be the case. Therefore one concludes that the theory described by Eq. (8) is not closed under renormalization. One must add more bare quartic operators (all differing by the function of  $z$  and  $z^*$  that they carry as a prefactor) to try to close the theory. These new operators will in turn generate their own family of new one-loop terms, until eventually one must admit that the theory naturally contains an infinite number of marginal quartic operators. The only systematic way to proceed is to generalize the theory in such a way that this infinite number of operators is simultaneously renormalized — this is achieved by the FRG.

The theory defined in Eq. (8) contains a local quartic coupling. To generalize this coupling as much as possible we consider a quartic interaction of the form

$$\int d^{d-2} r \int dz_1 dz_1^* dz_2 dz_2^* F(z_1, z_1^*, z_2, z_2^*) \phi_i^*(z_1^*, \mathbf{r}_\perp) \times \phi_i(z_1, \mathbf{r}_\perp) \phi_j^*(z_2^*, \mathbf{r}_\perp) \phi_j(z_2, \mathbf{r}_\perp).$$

[In principle one could mix the internal field labels  $i$  with the transverse plane positions, akin to the cubic anisotropy term that may be added to the standard  $O(N)$  model. We shall not consider such terms here.] As explicitly shown by BNT, under the combined translational and gauge symmetries, the general function  $F$  is constrained to have the form

$$F(z_1, z_1^*, z_2, z_2^*) = g(|z_1 - z_2|^2) \exp[-\mu^2(|z_1|^2 + |z_2|^2)]. \quad (12)$$

The original theory with local quartic interaction corresponds to the above coupling function  $g$  taking the form of a  $\delta$  function. To close the theory under renormalization has necessitated changing this  $\delta$  function to an *arbitrary* function. The one-loop terms in the perturbation expansion will now renormalize this function, and the usual flow equations for the coupling constants will take the form of nonlinear integro-differential equations.

To implement the FRG we must therefore start with a free energy functional of the form

$$F = \int d^{d-2} r_\perp \int dz dz^* e^{-\mu^2 |z|^2 / 2} (|\nabla_\perp \phi_i|^2 + \tau |\phi_i|^2) + \int d^{d-2} r_\perp \int dz_1 dz_1^* e^{-\mu^2 |z_1|^2 / 2} \times \int dz_2 dz_2^* e^{-\mu^2 |z_2|^2 / 2} g(|z_1 - z_2|^2) \times |\phi_i(z_1, \mathbf{r}_\perp)|^2 |\phi_j(z_2, \mathbf{r}_\perp)|^2. \quad (13)$$

We have somewhat sketched over the motivation of the functional form of the above free energy. The reader is referred to the original work of BNT for more details. Now that we have this functional form we shall describe the FRG in much more detail, principally because there are some subtleties which were previously overlooked.

In order to derive the functional flow equation ( $\beta$  functional) for the coupling function  $g$  it is necessary to evaluate the perturbative corrections to the form of the four-point correlator. At the bare level this function is simply the bare vertex which is now of the form  $-g(|z_1 - z_2|^2) \exp[-\mu^2(|z_1|^2 + |z_2|^2)/2]$ . At the level of one loop there are essentially four diagrams which contribute. In Appendix A we explicitly illustrate and evaluate these diagrams. Although the elegant analysis of BNT guarantees that the renormalization of the vertex is now closed, it is still rather difficult to extract the renormalization of the vertex. For this reason, it is necessary to introduce a representation of the coupling function  $g$  which makes the renormalization transparent. The choice of BNT was the following:

$$g(u) = \frac{1}{2} \int_0^\infty \frac{dx}{x} \rho(x) \exp[-(\mu^2/4x)u]. \quad (14)$$

So the FRG will now appear in the form of a flow equation for the ‘‘weight’’ function  $\rho(x)$ . There are three points we

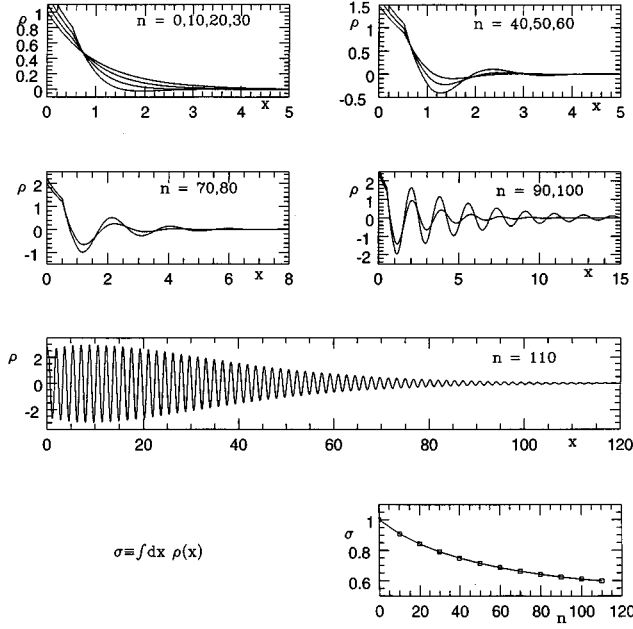


FIG. 1. The function  $\rho(x)$  under iteration for the case  $N \rightarrow \infty$  with  $\epsilon = 1$ . After  $n = 110$  iterations, the function has developed oscillations over a very large region. These ever-growing oscillations resemble a typical FRG flow instability, but the limit of  $N \rightarrow \infty$  is known to have a simple, stable FRG fixed point in other FRG representations. This is exemplified by following the integral  $\sigma$ , of  $\rho(x)$ , as a function of iteration number. It is clearly heading smoothly towards its fixed point value (equal to  $1/2$  for  $\epsilon = 1$ ).

wish to make at this juncture. First, the flow equation obtained for  $\rho(x)$  is extremely complicated. This may sound like a minor quibble, but in reality the solution of such an equation is highly nontrivial. Since the flow equation is bound to take the form of a nonlinear integro-differential equation, the simpler the form of the equation, the higher the chance of a satisfactory analysis. Second, and much more importantly, we must be sure that fixed point solutions for the “physical” coupling function also correspond to fixed point solutions for the representative function [in this case  $\rho(x)$ ]. Unfortunately, it turns out that the choice of BNT does not fulfil this requirement. As an example (we refer the reader to the next section for details) the solvable case of  $N \rightarrow \infty$  indeed has a stable fixed point for the coupling function  $g(u)$ . This solution is nontrivial, and takes the form of a distribution

$$g(|z_1 - z_2|^2) \sim \epsilon \delta^2(z_1 - z_2) \exp[-(\mu^2/2) \nabla_{x,y}^2].$$

Similarly, the case of  $N=0$  may also be shown to give a stable fixed point which is simply  $g(|z_1 - z_2|^2) = \text{const}$ . In each case the weight function  $\rho$  is ill defined, and any numerical attempt to find the fixed point from the flow equation for  $\rho$  will fail. We refer the reader to Fig. 1, where a numerical demonstration of the failure of the  $\rho(x)$  representation is given for the case  $N \rightarrow \infty$ . Third, we mention a more subtle point. The fixed point function may be expected to signal the physical transition from a vortex liquid to a vortex crystal. In this case, we shall lose the rotational invariance of the theory when we are in the low-temperature phase. Therefore, allow-

ing the coupling function to depend only on one variable, i.e.,  $u = |z_1 - z_2|^2$ , will preclude *a priori* any fixed points corresponding to the formation of a vortex crystal which, of course, breaks the rotational invariance implicit in the representation (14).

For these reasons it is necessary to make a new representation of the coupling function  $g$ . This new representation must fulfil the following conditions: (i) lead to a (numerically) tractable flow equation, (ii) be sensitive to all fixed points of the original coupling function, and (iii) be sensitive to the existence of a VLVC transition. It turns out that a representation is available which not only satisfies the above conditions, but which also has two more highly desirable features, namely, (i) allows some analytic treatment of the FRG flow equation and (ii) is directly related to a measurable physical quantity — the structure function for superconducting density-density correlations. After so much buildup, one is slightly embarrassed to reveal that this representation is nothing more than the Fourier transform of the original coupling function.

Explicitly, we define a function  $\tilde{f}(\mathbf{k})$  by

$$\tilde{f}(\mathbf{k}) = 2\mu^2 \tilde{g}(\mathbf{k}) \exp[-k^2/2\mu^2], \quad (15)$$

where  $\tilde{g}$  is the Fourier transform (FT) of  $g(x,y)$ . We stress that this FT is defined in the two dimensional  $(x,y)$  plane, so that the momentum  $\mathbf{k}$  is two-dimensional. We shall always use the momentum symbols  $\mathbf{k}$  and  $\mathbf{p}$  for momenta in the transverse plane. The momenta used for the (critical) transverse fluctuations are  $d-2$  dimensional and will always be denoted by  $\mathbf{q}_\perp$ .

We now refer the reader to Appendix A where a full derivation of the FRG flow equation is presented in terms of the new representation  $\tilde{f}$ . The resulting equation takes the form

$$\partial_t \tilde{f}(\mathbf{k}) = \epsilon \tilde{f} - (N/2) \tilde{f}^2 - 2\tilde{f} \circ \tilde{f} - 2\tilde{f} \tilde{f}^*, \quad (16)$$

where

$$\tilde{\alpha}(\mathbf{k}) \circ \tilde{\beta}(\mathbf{k}) \equiv \int \frac{d^2 p}{2\pi} \tilde{\alpha}(\mathbf{p}) \tilde{\beta}(\mathbf{k} - \mathbf{p}) \cos^2[(\mathbf{p} \times \mathbf{k})/2] \quad (17)$$

and

$$\alpha^*(\mathbf{k}) \equiv \int \frac{d^2 p}{2\pi} \tilde{\alpha}(\mathbf{p}) \cos(\mathbf{p} \times \mathbf{k}), \quad (18)$$

with the definition  $\mathbf{p} \times \mathbf{k} = p_x k_y - p_y k_x$  (we have also scaled wave vectors by  $\mu$ ).

The analysis of the above flow equation (together with the analogous equation for the disordered case) will occupy the remainder of this paper. Before proceeding with the analysis we shall conclude the present section by generalizing the flow equation to account for disorder.

Following the previous arguments of BNT concerning the generation of an infinite number of marginal quartic operators, the disorder quartic coupling introduced in Eq. (10) is also seen to require generalization to a coupling function. The free energy functional analogous to Eq. (13) with the inclusion of disorder is of the form

$$\begin{aligned}
F = & \int d^{d-2}r_{\perp} \int dz dz^* e^{-\mu^2|z|^2/2} (|\nabla_{\perp} \phi_i^{\alpha}|^2 + \tau |\phi_i^{\alpha}|^2) + \int d^{d-2}r_{\perp} \int dz_1 dz_1^* e^{-\mu^2|z_1|^2/2} \int dz_2 dz_2^* e^{-\mu^2|z_2|^2/2} g(|z_1 - z_2|^2) \\
& \times |\phi_i^{\alpha}(z_1, \mathbf{r}_{\perp})|^2 |\phi_j^{\beta}(z_2, \mathbf{r}_{\perp})|^2 - \int d^{d-2}r_{\perp} \int dz_1 dz_1^* e^{-\mu^2|z_1|^2/2} \int dz_2 dz_2^* e^{-\mu^2|z_2|^2/2} \Delta(|z_1 - z_2|^2) |\phi_i^{\alpha}(z_1, \mathbf{r}_{\perp})|^2 |\phi_j^{\beta}(z_2, \mathbf{r}_{\perp})|^2.
\end{aligned} \tag{19}$$

As before we are obliged to make a representation of the coupling functions  $g$  and  $\Delta$ . We again use the FT representation, and along with the previously introduced  $\tilde{f}$ , we define

$$\tilde{D}(\mathbf{k}) = 2\mu^2 \tilde{\Delta}(\mathbf{k}) \exp[-k^2/2\mu^2], \tag{20}$$

where  $\tilde{\Delta}$  is the Fourier transform of  $\Delta(x, y)$ . In Appendix B we illustrate the diagrams which contribute to the one-loop renormalization of the coupling functions  $\tilde{f}$  and  $\tilde{D}$ . The resulting flow equations take the form

$$\begin{aligned}
\partial_l \tilde{f}(\mathbf{k}) &= \epsilon \tilde{f} - (N/2) \tilde{f}^2 - 2\tilde{f} \circ \tilde{f} - 2\tilde{f} f^* + 4\tilde{f} \circ \tilde{D} + 2\tilde{f} D^*, \\
\partial_l \tilde{D}(\mathbf{k}) &= \epsilon \tilde{D} - N \tilde{D} \tilde{f} + 2\tilde{D} \circ \tilde{D} + 2\tilde{D} D^* - 2\tilde{D} f^*,
\end{aligned} \tag{21}$$

with the same notation as used above.

Finally, we shall briefly mention the form of the one-loop corrections to the propagator. These corrections contribute to the fixed point value of the correlation length exponent  $\nu$ . In Appendix C we illustrate the diagrams required to one loop, for both the pure and disordered cases. It is seen that these one-loop corrections have a particularly elegant form in terms of  $\tilde{f}$  and  $\tilde{D}$ . Explicitly we have<sup>13</sup> (to one-loop order)

$$2 - \frac{1}{\nu} = \frac{N}{2} \tilde{f}(\mathbf{0}) + f(\mathbf{0}) - D(\mathbf{0}), \tag{22}$$

where naturally  $f$  and  $D$  are the inverse Fourier transforms of the coupling functions  $\tilde{f}$  and  $\tilde{D}$ .

#### IV. SOLVABLE LIMITS

In this section we shall concentrate on direct analytic approaches to the FRG flow equation for the pure system, Eq. (16). For arbitrary values of  $N$  the flow equation is intractable, as it takes the form of a nonlinear integro-differential equation. However, the two extreme cases of  $N \rightarrow \infty$  and  $N=0$  may be treated exactly. We shall discuss these two limits below, with emphasis placed on the singular form of the corrections in each case.

##### A. $N \rightarrow \infty$

As is usual for large- $N$  calculations, it is first necessary to rescale the coupling (function) by  $N$ , prior to taking the limit of infinite  $N$ . So rescaling  $\tilde{f} \rightarrow 2\tilde{f}/N$  and taking  $N \rightarrow \infty$ , we have the flow equation

$$\partial_l \tilde{f} = \epsilon \tilde{f} - \tilde{f}^2. \tag{23}$$

This is a very simple equation and may be immediately integrated to give

$$\tilde{f}(\mathbf{k}, l) = \frac{\epsilon \tilde{f}(\mathbf{k}, 0) e^{\epsilon l}}{\epsilon + (e^{\epsilon l} - 1) \tilde{f}(\mathbf{k}, 0)}. \tag{24}$$

We see that as  $l \rightarrow \infty$  the function approaches the stable fixed point  $\tilde{f}_s(\mathbf{k}) = \epsilon$ , as long as the initial function is everywhere nonzero. The reader is encouraged to compare this result to that contained in a recent exact large- $N$  analysis for this same problem.<sup>7</sup> Contact between the two results may be made by regarding the FRG flow parameter  $l$  as related to the transverse momentum via  $q_{\perp} = e^{-l}$ . The finite  $N$  corrections are highly nontrivial to calculate for arbitrary dimension. However, our flow equation (16) is valid for all  $N$  to first order in  $\epsilon$ , and therefore we may easily study the finite- $N$  corrections within this one-loop level. A surprise is in store.

Let us concentrate purely on the fixed point, and denote the large- $N$  solution by  $w(\mathbf{k}) = \lim_{N \rightarrow \infty} \tilde{f}_s$ . We then write  $\tilde{f}'_s = w + (1/N) \tilde{f}'_s + O(1/N^2)$ . The correction to the large- $N$  fixed point  $\tilde{f}'_s$  is then given by the equation

$$0 = (\epsilon - 2w) \tilde{f}'_s - 4w \circ w - 4w w^*. \tag{25}$$

We now recall that  $w = \epsilon$ . It is seen that the term  $w \circ w$  in the above equation diverges as the system size (in the  $x, y$  directions)  $A$ . In other words, *the finite- $N$  corrections may not be considered as small in the thermodynamic limit*. The strict order of limits that one must take is first  $A \rightarrow \infty$  followed by  $N \rightarrow \infty$ . We see that for the large- $N$  limit to have meaning within this order of limits, we are forced to abandon our solution  $w = \epsilon$ . The correct solution must simultaneously solve the trivial equation  $w = w^2$  and also keep the integral  $w \circ w$  finite in the thermodynamic limit. One such type of solution is some sparse set of Kronecker  $\delta$  functions. The large- $N$  limit is not sophisticated enough to resolve the exact form of  $w$ , but we have the very interesting hint that the fixed point function may prefer to have some type of lattice structure (a lattice of Kronecker spikes in this case). In fact we can proceed a little further with this idea, anticipating somewhat the ideas to be presented in Sec. VI. Let us assume that the fixed point function chooses to take the form of some regular lattice of Kronecker spikes. We write this as

$$w(\mathbf{k}) = \frac{\epsilon}{\delta^2(\mathbf{0})} \sum_{\mathbf{G}} \delta^2(\mathbf{k} - \mathbf{G}), \tag{26}$$

where the reciprocal lattice vectors (RLV's)  $\{\mathbf{G}\}$  are as yet undetermined. We now look to the form of the  $1/N$  corrections. Referring to Eq. (25) we see that one of the contributions to  $\tilde{f}'_s$  is of the form  $w w^*$ . The function  $w^*$  is essentially the Fourier transform of  $w$ . We then see that there are only certain choices for the lattice constant of the RLV which will maintain the same functional form for the correc-

tion  $f'_s$  as compared to the large- $N$  result  $w$ . The lattice constant is fixed by demanding that  $w$  and  $w^\star$  be identical. This is guaranteed, for example, by either a square lattice with spacing  $a^2 = (2\pi)$  or alternatively a triangular lattice with spacing  $a^2 = 4\pi/\sqrt{3}$ . These lattices correspond to the square and triangular lattice solutions of the mean-field theory considered by Abrikosov.

We should point out that there exists a controversy in the literature concerning the correct theory of the large- $N$  limit within the LLL approximation. The author of Ref. 7 finds a continuous transition while the authors of Ref. 8 find the transition to be first order (for  $d < 6$ ). We believe that in the strictly infinite system the latter conclusion is valid and that the difference in results probably lies in the commutation of the  $N \rightarrow \infty$  limit and the thermodynamic limit, as demonstrated above from the one-loop FRG equation.

### B. $N \rightarrow 0$

In the strict limit of  $N=0$  the flow equation takes the form

$$\partial_t \tilde{f}(\mathbf{k}) = \epsilon \tilde{f} - 2\tilde{f} \circ \tilde{f} - 2\tilde{f} f^\star. \quad (27)$$

This equation is trivially solved at the fixed point by  $\tilde{f}(\mathbf{k})_s = (\pi\epsilon/2) \delta^2(\mathbf{k})$ . So the solutions of the infinite- $N$  and  $N=0$  limits are in total contrast, being a constant and a  $\delta$ -function, respectively. We see that the finite- $N$  fixed point (in particular  $N=2$ ) must in some sense be a natural compromise between these two forms. If one tries to expand about the above result in powers of  $N$ , then one finds that the  $O(N)$  corrections diverge with the system size. We have the same problem as encountered in the large- $N$  limit — the corrections are singular in the thermodynamic limit.

There are two approaches to the current difficulty. First, one may try some RLV solution to the  $N=0$  limit, and then see if the small- $N$  expansion is sensible. This is easily performed and one readily sees that the RLV solution does indeed exist in this limit, and is consistently “renormalized” by small- $N$  corrections, if one chooses the particular Abrikosov RLV mentioned above. An interesting alternative is to recognize that the small- $N$  behavior is not analytic and to make some scaling *Ansatz* to cope with this.

Consider the full flow equation (16) and make the rescaling  $\tilde{F}(\mathbf{k}) = N\tilde{f}(N^{1/2}\mathbf{k})$ . We then have explicitly

$$\begin{aligned} \partial_t \tilde{F}(\mathbf{k}) &= \epsilon \tilde{F}(\mathbf{k}) - (1/2) \tilde{F}^2 - 2 \\ &\times \int (d^2 p/2\pi) \tilde{F}(\mathbf{p}) \tilde{F}(\mathbf{k}-\mathbf{p}) \cos^2(N\mathbf{p} \times \mathbf{k}/2) \\ &- 2\tilde{F}(\mathbf{k}) \int (d^2 p/2\pi) \tilde{F}(\mathbf{p}) \cos(N\mathbf{p} \times \mathbf{k}). \end{aligned} \quad (28)$$

Now taking  $N \rightarrow 0$  in the above equation for  $\tilde{F}$  produces the small- $N$  form for the original function  $\tilde{f}$ , as the scaling *Ansatz* and the limit  $N \rightarrow 0$  do not commute. In this way we are able to examine the nonanalytic small- $N$  behavior of the coupling function. Taking the limit  $N \rightarrow 0$  in the above equation simply removes the trigonometric terms. With suitable rescalings of  $\tilde{F}$  and momentum, the fixed point of the flow equation is determined by the appealingly simple equation

$$\tilde{F}(\mathbf{k}) = \tilde{F}(\mathbf{k})^2 + \int (d^2 p/2\pi) \tilde{F}(\mathbf{p}) \tilde{F}(\mathbf{k}-\mathbf{p}). \quad (29)$$

In other words we require a function which is equal to the sum of its square and its self-convolution. This problem has proved to be extremely nontrivial, and we consider it worthy of study in its own right.

This is not the place for an extended discussion of this equation. However, we shall make a few points. First, we note that the RLV *Ansatz* provides a whole class of solutions to the above problem. In other words, Eq. (29) is solved by any regular lattice of Kronecker  $\delta$  functions (or appropriately normalized Dirac  $\delta$  functions) — there is no selection of lattice spacing. Second, we notice that a condition of solution is that if a particular function satisfies Eq. (29), then its Fourier transform must also satisfy the equation (since the form of the equation is invariant under a FT). The Abrikosov RLV solutions are then seen as somewhat special as they automatically fulfill this condition, being self-reciprocal under a FT. As a final point of interest, we may mention the results of a numerical study of the one-dimensional analog of the above equation. We consider the equation

$$f(x) = f(x)^2 + (2\pi)^{-1/2} \int_{-\infty}^{\infty} dy f(y) f(x-y). \quad (30)$$

In the next section we shall give details of some numerical attempts to solve the full flow equation. One of the methods used was a Newton root-finding algorithm (see Sec. V for details). The application of this method to the above equation produced astonishing results. There appear to be an infinite number of *localized* solutions to Eq. (30). A given solution is selected according to the initial guess fed into the Newton algorithm. The solutions are stable to changes in the discrete grid size, and are therefore not artifacts of the grid. We show in Fig. 2 an example of one of these localized solutions, together with its self-convolution, so that the reader may appreciate the delicate balance achieved by the function in creating “windows” within itself so as to reduce its self-convolution in the tails of the function.

## V. NUMERICAL ANALYSIS

In the previous section we have described our attempts at direct analytic solution of the flow equation. We have seen that for  $N \rightarrow \infty$  and  $N=0$ , simple solutions are possible, but that the corrections are singular in each case, as they diverge with the system size. Since we are really interested in  $N=2$ , which corresponds to the original model for the superconductor, we have to resort to some numerical procedure in order to solve the flow equation. (We remind the reader that our main results will in fact be discussed in the next two sections where we use a physically motivated *Ansatz* to extract results from the flow equation.)

A numerical analysis of the FRG flow equation is an extremely nontrivial task as Eq. (16) takes the form of a nonlinear, two-dimensional, integro-differential equation. We have employed two different numerical techniques in an attempt to solve the equation. The first technique is a simple iteration scheme (also used in the original work of BNT), implemented by discretizing momentum space  $\mathbf{k}$  and the flow variable  $l$ . For a given iteration step (proportional to

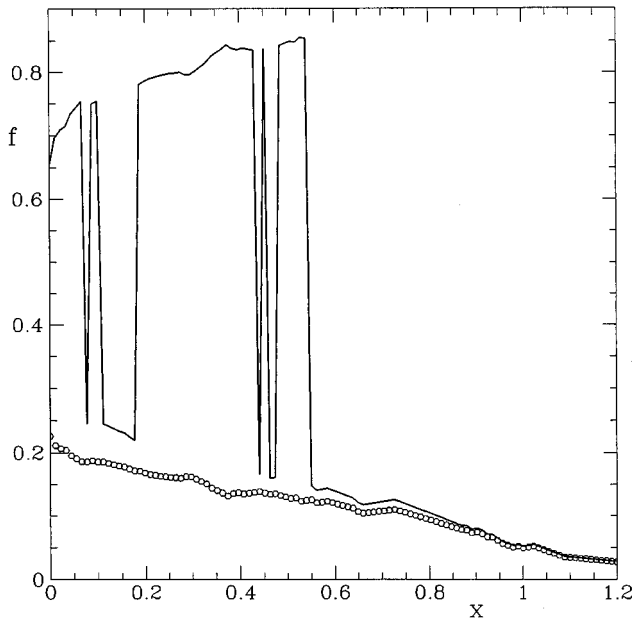


FIG. 2. One of the infinitely many localized solutions of Eq. (30). The function  $f(x)$  is given by the solid line, while the circles represent the self-convolution of  $f(x)$ . Note how the function creates “windows” within itself, so as to lessen its self-convolution in the tails of the function.

$l$ ) one evaluates the integrals on the right-hand side (RHS) of the flow equation, and therefore determines (within some precision) the form of the function  $f(\mathbf{k}, l)$  at the next iteration step. One can improve the numerical stability of this procedure by using Runge-Kutta algorithms.<sup>14</sup> In following the flow of the equation in such an iterative manner, it is crucial to make a good initial “guess” for the function. If one starts too far away from a (possible) fixed point, then the cumulative errors picked up through iteration may well destabilize the scheme before one has got close to the fixed point. For all choices of initial guess, we were unable to find any stable fixed point. The generic behavior of the function under iteration is to develop propagating oscillations whose amplitudes grow exponentially fast. Within some finite time, the function becomes nonnegligible at the grid boundary, and one is obliged to halt the procedure. The runaway of the function bears some similarity to that portrayed for the BNT weight function in Fig. 1 [although we should point out once more that instabilities in the coupling function  $\rho(x)$  which are present in the case of  $N \rightarrow \infty$  are spurious, since this case supports the stable fixed point  $\tilde{f} = \epsilon$ ].

A more attractive numerical procedure is that of “root finding” using a simple Newton scheme.<sup>14</sup> One works directly at the fixed point, and therefore solves Eq. (16) with the LHS set equal to zero. By discretizing the momentum space, one may regard the fixed-point equation as a large number of coupled algebraic equations. The solution of such a problem may then be regarded as a root-finding exercise and one may employ the Newton algorithm.<sup>14</sup> This procedure is also sensitive to the original guess of the “roots,” as the Newton scheme is notoriously unstable if one starts too far away from the true solution. By using this method we were successful in finding many fixed point solutions of Eq. (16). In fact we believe there to be an infinite number of such

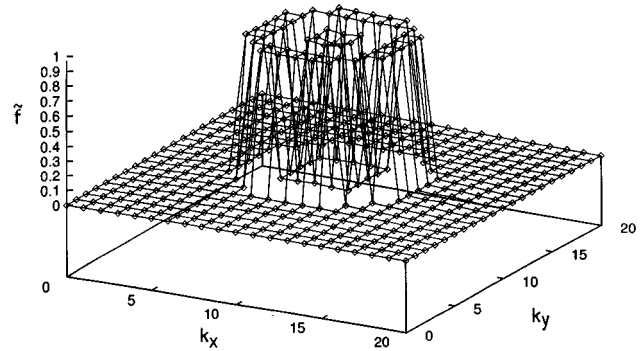


FIG. 3. An example of one of the infinitely many unstable fixed points (found by use of the Newton root-finding scheme) for the coupling function  $\tilde{f}(\mathbf{k})$  in the absence of disorder.

solutions. In Fig. 3 we present a typical example of such a fixed point — its cross section bears a similarity to the one-dimensional solution of the small- $N$  problem discussed in the previous section. The remaining difficulty with generating fixed point solutions using the Newton method is that one has no information concerning their stability, whereas the iteration method only finds stable fixed points by construction. To check the stability of the solutions found by the Newton method one has several possibilities. One method is to simply diagonalize the stability matrix of the system of equations and examine the eigenvalue spectrum. Alternatively, one may insert the fixed point solution into the iteration algorithm and study the evolution — a stable fixed point will not evolve. Unfortunately we report that all of the solutions we found using the Newton method proved to be unstable.

We repeated all of the above numerical analysis for the coupled flow equations containing the disorder function  $\tilde{D}$ . The generic behavior of the iteration method was rather similar to that described above for weak disorder strength (i.e., small initial guess for  $\tilde{D}$ ). For larger values of  $\tilde{D}$ , the flow was still unstable, but in a different way. In contrast to the previous case where the functions became unstable by developing ever-growing oscillations, in this case, the instability was characterized by the function simply growing in size, with no oscillatory structure appearing. Again, the iteration was abandoned when the functions became nonnegligible at the grid boundary.

The main results of our numerical analysis of the flow equations is that (i) iteration of smooth functions invariably leads to instabilities and (ii) the flow space is extremely complicated as it contains an infinite number of unstable fixed points. The open question remains, of course, are there any stable fixed points?

## VI. RLV ANSATZ

From the last two sections, a rather forlorn picture has emerged. The solvable limits of  $N \rightarrow \infty$  and  $N = 0$  have been singular, so that no systematic expansion has been possible, and the numerical analysis of the flow equation has yielded no conclusive results as to the existence of stable FRG fixed points. In such a situation, an *Ansatz* is required.

The one positive result we obtained from analyzing the

solvable limits was that the flow equation contained information about the Abrikosov lattice. This was clear from the large- $N$  limit, where we found that the only solution which was well defined in the thermodynamic limit was one possessing a lattice structure and that the Abrikosov lattice was selected by studying the finite- $N$  corrections. It is then natural to try to *construct* a fixed point solution for arbitrary  $N$  by considering solutions which are expressed in terms of a reciprocal lattice, bearing in mind that the lattice is likely to be that of Abrikosov.

Let us first consider the case without disorder — we refer the reader to the relevant flow equation (16) in Sec. III. We make the RLV *Ansatz*

$$\tilde{f}(\mathbf{k}) = \sum_{\mathbf{G}} A(\mathbf{G}) \delta^2(\mathbf{k} - \mathbf{G}), \quad (31)$$

where the vectors  $\{\mathbf{G}\}$  are a set of RLV's, but with no more precise specification as yet. Inserting this *Ansatz* into the flow equation yields the interesting result that no new terms are generated if the RLV is chosen to be of Abrikosov form. More specifically, the RLV must be self-reciprocal under a FT, implying (for example) either a triangular lattice of spacing  $a$ , with  $a^2 = 4\pi/3$ , or else a square lattice with spacing  $a$ , satisfying  $a^2 = 2\pi$ . In other words, this form of the coupling function is *closed* under renormalization.

There are several points to be made in relation to the RLV *Ansatz*. The first such point was already made in Sec. III. Since we are hoping to describe the VLVC transition, we may expect the coupling function to take a fixed point form which breaks rotational invariance, such as the RLV form. Another point to consider is the meaning of the runaway flows found numerically for initial guesses of the coupling function which were smooth functions. Although one may regard these flows as signaling a first-order transition, this is based more on prejudice than anything else. It is equally possible that the flow is simply heading towards a strong-coupling fixed point. We regard the RLV *Ansatz* as the correct form of the coupling function at this strong-coupling fixed point. In other words, the correct “ $\phi^4$ ” theory for this system is such that the coupling function takes nonzero values only at values of momentum which are coincident with a vector of a reciprocal lattice. Of course such a model cannot describe the liquid phase. In that respect it is similar to some of the theories of two-dimensional melting which, being expressed in terms of Burgers vectors, can only in a straightforward way describe the crystalline phase (see, e.g., Nelson and Halperin<sup>15</sup>). While we have been unable to derive this RLV model starting from Eq. (13), we feel it captures the essence of the symmetries broken in the transition and hence because of “universality” arguments provides a way of calculating critical exponents, etc., at the transition, should it be a continuous one. Strong support for the RLV model is provided by the work of Yeo and Moore<sup>16</sup> where the function  $\tilde{f}(\mathbf{k})$  has been studied in the pure case in two dimensions within the well-known strong-coupling approximation in which all the parquet diagrams are summed. At criticality (which in this approximation is at zero temperature)  $\tilde{f}(\mathbf{k})$  has the RLV form.

For the full model including disorder, we make the simultaneous *Ansätze*

$$\tilde{f}(\mathbf{k}) = \sum_{\mathbf{G}} A(\mathbf{G}) \delta^2(\mathbf{k} - \mathbf{G}),$$

$$\tilde{D}(\mathbf{k}) = \sum_{\mathbf{G}} B(\mathbf{G}) \delta^2(\mathbf{k} - \mathbf{G}). \quad (32)$$

In the next section we shall study the fixed point properties associated with such a form for the coupling functions.

## VII. FIXED-POINT SOLUTIONS

One finds that the flow equations are immensely simplified by our particular choice of the RLV — the RLV of the Abrikosov lattice. For this choice the trigonometric terms in the convolution-type integrals become equal to unity, and the functions  $\tilde{f}$  and  $\tilde{D}$  become self-reciprocal under the FT. Proceeding with this choice of the RLV, it is possible to make analytic progress with the simple *Ansatz*  $A(\mathbf{G})=A$ ,  $B(\mathbf{G})=B$ , i.e., choosing the RLV coefficients to be independent of  $\mathbf{G}$ .

We shall proceed to derive the fixed points and their associated stability eigenvalues in some detail, for the disordered case. Given the coupled flow equations (21) we make the *Ansätze*

$$\tilde{f}(\mathbf{k}) = A \sum_{\mathbf{G}} \delta^2(\mathbf{k} - \mathbf{G}),$$

$$\tilde{D}(\mathbf{k}) = B \sum_{\mathbf{G}} \delta^2(\mathbf{k} - \mathbf{G}), \quad (33)$$

where we choose the reciprocal lattice to be a square lattice of spacing  $a = (2\pi)^{1/2}$ . This particular choice is purely for convenience. At this one-loop level, the only relevant characteristic of the reciprocal lattice is its self-reciprocity under a FT. Therefore the square lattice with spacing  $a = (2\pi)^{1/2}$  and the triangular lattice with spacing  $a = (4\pi/3)^{1/2}$  will have the same FRG properties.

As an example of how to calculate the terms in the flow equations with this form of the coupling functions, consider the convolution term  $\tilde{f} \circ \tilde{f}$ , defined explicitly in Eq. (17):

$$\begin{aligned} \tilde{f} \circ \tilde{f} &= A^2 \sum_{\mathbf{G}} \sum_{\mathbf{G}'} \int \frac{d^2p}{2\pi} \delta(\mathbf{p} - \mathbf{G}) \delta^2(\mathbf{k} - \mathbf{p} - \mathbf{G}') \\ &\quad \times \cos^2\left(\frac{1}{2}\mathbf{p} \times \mathbf{k}\right) \\ &= \frac{A^2}{2\pi} \sum_{\mathbf{G}} \sum_{\mathbf{G}'} \delta^2(\mathbf{k} - \mathbf{G}'). \end{aligned} \quad (34)$$

We must fix the value of the free sum over reciprocal lattice vectors. This is conveniently done by considering the RLV sum over  $\exp(i\mathbf{k} \cdot \mathbf{G})$ . We have

$$\begin{aligned}
\sum_{\mathbf{G}} \exp(i\mathbf{k} \cdot \mathbf{G}) &= \sum_{m,n} \exp(ik_x ma + ik_y na) \\
&= (2\pi)^2 \sum_{m',n'} \delta(k_x a - 2\pi m') \delta(k_y a - 2\pi n') \\
&= \frac{(2\pi)^2}{a^2} \sum_{\mathbf{G}} \delta^2(\mathbf{k} - \mathbf{G}) = 2\pi \sum_{\mathbf{G}} \delta^2(\mathbf{k} - \mathbf{G}).
\end{aligned} \tag{35}$$

Setting  $\mathbf{k}=\mathbf{0}$  in the above we see that  $\Sigma_{\mathbf{G}}=2\pi\delta^2(\mathbf{0})$ . Returning to Eq. (34) we then have

$$\tilde{f} \circ \tilde{f} = A^2 \delta^2(\mathbf{0}) \sum_{\mathbf{G}} \delta^2(\mathbf{k} - \mathbf{G}). \tag{36}$$

Similar manipulations with the other terms in Eq. (21) then yield the flow equations for  $A$  and  $B$ :

$$\begin{aligned}
\partial_l A &= \epsilon A - [(N/2)A^2 + 2A^2 + 2A^2 - 4AB - 2AB] \delta^2(\mathbf{0}), \\
\partial_l B &= \epsilon B - [NAB - 2B^2 - 2B^2 + 2AB] \delta^2(\mathbf{0})
\end{aligned} \tag{37}$$

[where we have kept all the contributions separate to allow easy cross-reference with the original flow equation (21)].

One easily finds fixed point values for  $A$  and  $B$ , leading to fixed point solutions for the coupling functions of the form

$$\begin{aligned}
\tilde{f}_s &= \frac{\epsilon}{2(N-1)\delta^2(\mathbf{0})} \sum_{\mathbf{G}} \delta^2(\mathbf{k} - \mathbf{G}), \\
\tilde{D}_s &= \frac{(4-N)\epsilon}{8(N-1)\delta^2(\mathbf{0})} \sum_{\mathbf{G}} \delta^2(\mathbf{k} - \mathbf{G}).
\end{aligned} \tag{38}$$

The allowed range of the parameter  $N$  is now  $1 < N < 4$ , in order to ensure the nonnegativity of the coupling functions.

The one-loop correction to the correlation length exponent is given by  $2 - 1/\nu = (N/2)\tilde{f}(0) + f(0) - D(0)$ , and we therefore have at the above fixed point

$$\frac{1}{\nu} = 2 - \frac{3N}{8(N-1)} \epsilon + O(\epsilon^2). \tag{39}$$

To address the question of stability of this fixed point, we consider perturbations to the coupling functions. In order to remain within the space of coupling functions consistent with the RLV model, the perturbations must in turn be restricted to the RLV. We write  $\tilde{f} = \tilde{f}_s + \tilde{\eta}$  and  $\tilde{D} = \tilde{D}_s + \tilde{\xi}$  with the explicit definitions

$$\begin{aligned}
\tilde{f}(\mathbf{k}, l) &= \tilde{f}_s(\mathbf{k}) + \sum_{\mathbf{G}} \alpha(\mathbf{G}, l) \delta^2(\mathbf{k} - \mathbf{G}), \\
\tilde{D}(\mathbf{k}, l) &= \tilde{D}_s(\mathbf{k}) + \sum_{\mathbf{G}} \beta(\mathbf{G}, l) \delta^2(\mathbf{k} - \mathbf{G}).
\end{aligned} \tag{40}$$

In terms of these perturbations we have the flow equations

$$\begin{aligned}
\partial_l \tilde{\eta} &= \epsilon \tilde{\eta} - N\tilde{f}_s \tilde{\eta} - 4\tilde{f}_s \circ \tilde{\eta} - 2\tilde{f}_s \eta^* - 2f_s^* \tilde{\eta} + 4\tilde{f}_s \circ \tilde{\xi} \\
&\quad + 4\tilde{D}_s \circ \tilde{\eta} + 2\tilde{f}_s \xi^* + 2D_s^* \tilde{\eta}, \\
\partial_l \tilde{\xi} &= \epsilon \tilde{\xi} - N\tilde{f}_s \tilde{\xi} - N\tilde{D}_s \tilde{\eta} + 4\tilde{D}_s \circ \tilde{\xi} + 2\tilde{D}_s \xi^* \\
&\quad + 2D_s^* \tilde{\xi} - 2\tilde{D}_s \eta^* - 2f_s^* \tilde{\xi}.
\end{aligned} \tag{41}$$

Calculating the momentum integrals in the above equations, we may write the flow equations in terms of the RLV coefficients  $\alpha$  and  $\beta$ :

$$\begin{aligned}
\partial_l \alpha &= \alpha [\epsilon - (N+2)A \delta^2(\mathbf{0}) + 2B \delta^2(\mathbf{0})] - 2\Sigma_1 [3A - 2B] \\
&\quad + 6\Sigma_2 A, \\
\partial_l \beta &= \beta [\epsilon - (N+2)A \delta^2(\mathbf{0}) - 2B \delta^2(\mathbf{0})] - NB \delta^2(\mathbf{0}) \alpha - 2\Sigma_1 B \\
&\quad + 6\Sigma_2 B,
\end{aligned} \tag{42}$$

where we have defined

$$\begin{aligned}
2\pi\Sigma_1(l) &\equiv \sum_{\mathbf{G}} \alpha(\mathbf{G}, l), \\
2\pi\Sigma_2(l) &\equiv \sum_{\mathbf{G}} \beta(\mathbf{G}, l).
\end{aligned} \tag{43}$$

To analyze these equations we first sum each equation over the RLV. This yields two coupled equations for the quantities  $\Sigma_1$  and  $\Sigma_2$  which we write in the form

$$\partial_l \Sigma_i = \Gamma_{i,j} \Sigma_j, \quad i, j = 1, 2, \tag{44}$$

where the matrix  $\Gamma$  has the form

$$\Gamma = \frac{\epsilon}{8(N-1)} \begin{pmatrix} -2(N+8) & 24 \\ -(N+2)(4-N) & 4(4-N) \end{pmatrix}. \tag{45}$$

The two eigenvalues of this matrix are found to be

$$\lambda_1 = -\frac{(4-N)\epsilon}{4(N-1)}, \quad \lambda_2 = -\epsilon. \tag{46}$$

Both eigenvalues are negative only when  $1 < N < 4$ . Therefore we see that for this range of  $N$ , the quantities  $\Sigma_i$  will decay exponentially fast to zero under the flow of the FRG.

We may therefore neglect  $\Sigma_1$  and  $\Sigma_2$  in the flow Eqs. (42). It is then easy to see that  $\alpha$  evolves according to

$$\partial_l \alpha = -\frac{(4-N)\epsilon}{4(N-1)} \alpha \tag{47}$$

and therefore decays exponentially fast to zero for  $1 < N < 4$ , with decay rate equal to the stability eigenvalue  $|\lambda_1|$ . Finally, neglecting  $\alpha$  in the flow equation for  $\beta$  we see that  $\beta$  also decays to zero in exponential fashion for  $1 < N < 4$ , again with decay rate equal to  $|\lambda_1|$ . So we conclude that the fixed-point solutions  $\tilde{f}_s$  and  $\tilde{D}_s$  given in Eqs. (38) are stable against arbitrary RLV perturbations in the parameter range  $1 < N < 4$  (which encompasses the physical case of  $N=2$  for the superconductor).

Interestingly, the value of the correlation length exponent and the value of the stability eigenvalues  $\lambda_1$  and  $\lambda_2$  (which are related to correction-to-scaling exponents) are the same

as those obtained for the simple  $O(N)$  model in the presence of disorder,<sup>11</sup> but in two dimensions lower. (Note that in this article  $\epsilon = 6 - d$ .)

One may also use this RLV *Ansatz* in the absence of disorder, i.e. Eq. (16). Performing precisely analogous steps to those outlined above, one finds the following results. One obtains a fixed point solution

$$\bar{f}_s = \frac{2\epsilon}{(N+8)\delta^2(\mathbf{0})} \sum_{\mathbf{G}} \delta^2(\mathbf{k}-\mathbf{G}), \quad (48)$$

The value of  $\nu$  at this fixed point is given by

$$\frac{1}{\nu} = 2 - \frac{(N+2)}{(N+8)}\epsilon + O(\epsilon^2), \quad (49)$$

identical with that obtained from the pure  $O(N)$  model<sup>17</sup> [again in two lower dimensions, i.e., a pure  $O(N)$  model with  $\epsilon = 4 - d$ ]. The stability analysis for the pure case reveals an eigenvalue spectrum characterized by two different eigenvalues, with values

$$\lambda_1 = \frac{(4-N)\epsilon}{4(N+8)}, \quad \lambda_2 = -\epsilon. \quad (50)$$

Clearly the fixed point is only stable for  $N > 4$ , and one may therefore not make the direct connection to the pure  $O(N)$  model, since  $N=4$  plays no special role in that case. [Intriguingly, the value of the eigenvalues for the pure superconductor are the same as those for the Heisenberg fixed point in the disordered  $O(N)$  model.<sup>11</sup>]

## VIII. DISCUSSION AND CONCLUSIONS

We now turn to the implications of our calculations. For  $N=2$  in the presence of disorder they suggest that our problem is in the same universality class as the disordered  $O(N)$  model in two dimensions lower. Thus, in the presence of disorder, one would not expect there to be a phase transition below four dimensions to a state with both off-diagonal long-range order (ODLRO) and crystalline order. This result is consistent with the old argument of Larkin<sup>18</sup> which shows that disorder removes crystalline order below four dimensions. It suggests that if there is a phase transition in three dimensions from the vortex liquid state to some other state, then this state cannot be crystalline, but must be a form of vortex ‘slush’ in which the crystalline order only exists over a finite length scale and that at the transition there is a jump in the degree of short-range crystalline order.

In the absence of disorder, we have been unable to find for  $N=2$  any stable fixed points even within the RLV model, and deduce that the original conclusion of BNT that the transition becomes first order below six dimensions is likely to be correct. One of us has shown<sup>19</sup> that thermal excitation of phase fluctuations does not permit the simultaneous existence of ODLRO and the vortex lattice for  $d < 4$  for the pure case. Thus it seems likely that 4 is a special dimension for both pure and disordered systems.

The recent magnetization measurements of Zeldov *et al.*,<sup>20</sup> on Bi-Sr-Ca-Cu-O provide very strong evidence that a first-order transition line exists. A striking feature of their data is that the line in the  $H$ - $T$  diagram (across which there is

a jump in the magnetization) seems to terminate at a critical end point at finite  $H$  and nonzero temperature. If these results are confirmed, it means that the low-temperature phase has the same symmetries as the normal vortex liquid as one can pass between the two around the critical end point without crossing a phase line — just as in the conventional liquid-gas transition. Thus the phase transition would indeed seem to be between a normal liquid region and a ‘vortex slush’ region, in which there exists ‘long’ short-range crystalline order. A low-temperature phase of this character was suggested in Ref. 19.

There is much experimental evidence also for a first-order transition in untwinned crystals of Y-Ba-Cu-O (e.g., Safar *et al.*<sup>21</sup>). Most of the experiments are transport measurements which show that there is a line in the  $H$ - $T$  diagram at which there is a sharp drop in the resistivity. This kink in the magnetoresistance becomes smeared at higher fields and the finite-resistivity curve displays Ohmic behavior.<sup>22</sup> Going to higher fields increases the effective strength of the disorder so that the direct introduction of point disorder via electron irradiation would be expected to mirror the effects seen in high fields. Fendrich *et al.*,<sup>23</sup> found that electron irradiation led to a suppression of the drop and a temperature dependence for the resistivity appropriate to a vortex liquid (with no evidence for a vortex glass transition). It seems possible that if the complications produced in Y-Ba-Cu-O by the strong hysteresis effects could be removed, then the resulting phase diagram might be similar to that found by Zeldov *et al.*, for Bi-Sr-Ca-Cu-O.

To what extent are our results consistent with these experimental findings? Our most important result is in the presence of disorder one does not expect there to be a low-temperature phase with long-range order of either the phase (ODLRO) or the density (crystalline order). Furthermore, if one rather boldly assumes that no other phases exist below four dimensions in the presence of weak disorder (strong disorder might be needed to produce gauge glass behavior), then the argument of Moore<sup>19</sup> for the pure case and that of Larkin<sup>18</sup> for the case of point disorder would imply that the low-temperature phase can only be of the ‘vortex slush’ variety and a phase diagram involving a critical end point should then be of little surprise. Of course, the form of the actual first-order line in the  $H$ - $T$  diagram is likely to depend on the amount of disorder present, the anisotropy, etc., in a way which is not directly obtainable from a RG calculation of the type used in this paper, which is only really useful for describing continuous phase transitions.

In fact, if the phase diagram of Zeldov *et al.* is generally valid, the only continuous transition is that associated with the critical end point itself. The order parameter associated with the transition is a scalar (it is essentially  $|\psi|^2$  whose thermal average is proportional to the magnetisation). Hence the critical exponents associated with the critical end point would be expected to be those of the random field Ising model as the disorder is coupled directly to the order parameter. (We are indebted to D.S. Fisher for this observation.) Since the exponent  $\beta$  of the random field model is extremely close to zero,<sup>24</sup> this would explain why at the end point the magnetization jump did not apparently go to zero.

ACKNOWLEDGMENTS

It is a pleasure to thank Alan Bray, Thomas Nattermann, Leo Radzihovsky, and Martin Zirnbauer for useful discussions. T.J.N. acknowledges financial support from EPSRC and SFB 341.

APPENDIX A

In this first appendix we shall present a detailed derivation of the FRG flow equation (16) for the case of no disorder. From the form of the free energy functional (13) we see that the bare propagator has the form

$$\sigma(\mathbf{q}_\perp; z_1^*, z_2) = \frac{1}{(q_\perp^2 + \tau)} \frac{\mu^2}{2\pi} \exp(\mu^2 z_1^* z_2 / 2), \quad (A1)$$

while the bare vertex [which is now a function of the  $(x, y)$ -plane coordinates] is given by

$$-g(|z_1 - z_2|^2) \exp[-\mu^2(|z_1|^2 + |z_2|^2)]. \quad (A2)$$

These diagrammatic elements are illustrated in Fig. 4. We shall be using standard dimensional regularization (in  $\epsilon = 6 - d$ ) along with the minimal subtraction method.<sup>12</sup> Therefore, from one-loop perturbation theory we shall attain a renormalization of the vertex of the symbolic form

$$g_R(s) = g(s) + (1/\epsilon) \int ds_1 ds_2 F(s, s_1, s_2) g(s_1) g(s_2) + O(g^3). \quad (A3)$$

The prefactor of  $1/\epsilon$  just comes from the integral over the internal transverse momenta (of dimension  $d - 2$ ), whereas the nontrivial kernel  $F$  is obtained by considering the internal integration over the ‘‘plane’’ variables.

To see how we arrive at such a renormalization of the vertex, consider the perturbative calculation of the four-point correlation function

$$C_4(\mathbf{q}_1, z_1; \mathbf{q}_2, z_2; \mathbf{q}_3, z_3^*; \mathbf{q}_4, z_4^*) \equiv \langle \phi_i(\mathbf{q}_1, z_1) \phi_j(\mathbf{q}_2, z_2) \phi_i^*(\mathbf{q}_3, z_3^*) \phi_j^*(\mathbf{q}_4, z_4^*) \rangle.$$

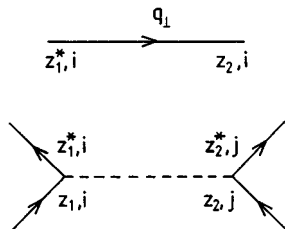


FIG. 4. The two basic diagrammatic elements used in the perturbation expansion: the propagator  $\sigma(\mathbf{q}_\perp; z_1^*, z_2)$  and the bare vertex.

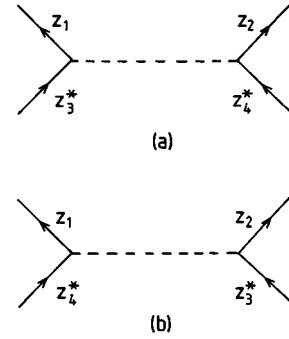


FIG. 5. The bare four-point correlation function  $C_{4,\text{bare}}$  — particular attention must be paid to distinguishing the two symmetry channels (a) and (b).

The first point to make is that we must be careful to distinguish between two different ‘‘symmetry channels’’ [denoted by (a) and (b)] which exist for this function. Since the vertex is nonlocal, we have two distinct pairings of the plane variables  $(z_1, z_2, z_3^*, z_4^*)$ , as shown in Fig. 5. When we come to evaluate the one-loop corrections, our representation must be such that there is an unambiguous renormalization of a given symmetry channel from a given one-loop diagram. (Such an unambiguous renormalization is not available within the representation of BNT — the question of whether this invalidates their flow equation is not presently clear.)

Before evaluating the bare diagrams, we must choose a representation for the vertex function  $g$ . As mentioned in the main text, we shall work with the Fourier transform of this function

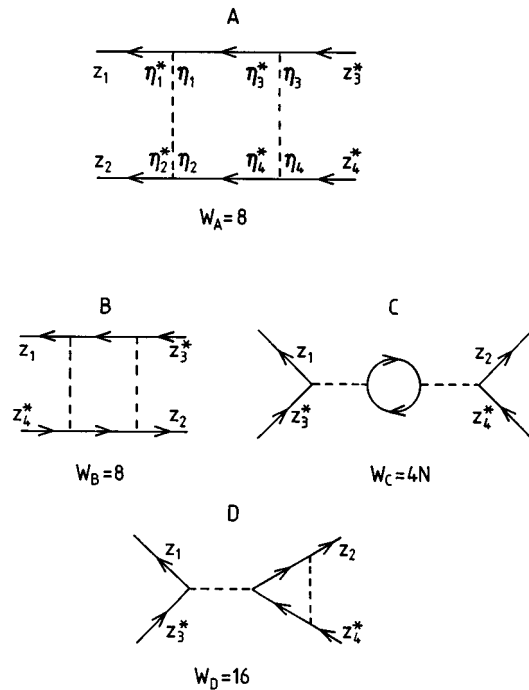


FIG. 6. The four one-loop contributions to  $C_4^a$ , along with their combinatoric weights. We have indicated the internal plane labels in the first diagram to allow comparison with Eq. (A5).

$$\tilde{g}(\mathbf{k}) = (1/2\pi) \int d^2r g(\mathbf{r}) e^{i\mathbf{k}\cdot\mathbf{r}}. \quad \tilde{g}(K) = (1/2\pi) \int dz dz^* g(z, z^*) \exp[i(K^*z + Kz^*)/2].$$

It is convenient to reexpress this FT in terms of complex momenta  $K = k_x + ik_y$  as

The bare diagram (a) may then be evaluated to give (up to a factor of the transverse parts of the four external propagators)

$$C_{4,\text{bare}}^a = -2 \left( \frac{\mu^2}{2\pi^2} \right) \exp \left[ \frac{\mu^2(z_1 z_3^* + z_2 z_4^*)}{2} \right] \int \frac{dK dK^*}{2\pi} \tilde{g}(K, K^*) \exp \left[ -\frac{KK^*}{\mu^2} - \frac{iK^*(z_1 - z_2)}{2} - \frac{iK(z_3^* - z_4^*)}{2} \right]. \quad (\text{A4})$$

The reader may be confused that we are not calculating the usual one-particle-irreducible functions. It is necessary in this calculation to attach the external propagators in order to give an identifiable ‘‘plane’’ label to each leg of the vertex. The transverse momentum part of the external propagators is irrelevant to the calculation and will be omitted. The expression for the bare diagram (b) may be obtained by interchanging  $z_1$  and  $z_2$  (or equivalently  $z_3^*$  and  $z_4^*$ ).

In Fig. 6 we show the four one-loop diagrams which will renormalize the bare diagram in channel A. (The diagrams contributing to channel B may be obtained by interchanging the labels  $z_1$  and  $z_2$ .) All these diagrams contain an identical internal integral over the transverse momenta. This integral has the form

$$\int \frac{d^{d-2}q_\perp}{(2\pi)^{d-2}} \frac{1}{(q_\perp^2 + \tau)} \frac{1}{[(\mathbf{q}'_\perp + \mathbf{q}_\perp)^2 + \tau]}$$

and has a singular contribution equal to  $S_{d-2}/\epsilon$  [where  $S_d$  is the surface area of a unit hypersphere in  $d$  dimensions, divided by  $(2\pi)^d$ ]. The constant  $S_{d-2}$  may be absorbed into the coupling function and will henceforth be omitted.

The internal integrals over the plane variables may be most easily done using the following formula for Gaussian integrals:

$$\int d^n z d^n z^* \exp[-\mu^2(z_i^* M_{ij} z_j - a_i^* z_i - z_i^* b_i)] = (\pi/\mu^2)^n (\det M)^{-1} \exp(\mu^2 a_i^* M_{ij}^{-1} b_j).$$

We shall follow the evaluation of diagram A rather closely, and then simply quote the results for the remaining three diagrams. So referring to diagram A, we have the explicit expression

$$\begin{aligned} \epsilon C_{4,A}^a &= \frac{(-1)^2 w_A}{2!} \left( \frac{\mu^2}{2\pi} \right)^6 \int d\eta_1 d\eta_1^* \cdots d\eta_4 d\eta_4^* \exp[\mu^2(|\eta_1|^2 + |\eta_2|^2 + |\eta_3|^2 + |\eta_4|^2)/2] g(|\eta_1 - \eta_2|^2) \\ &\quad \times g(|\eta_3 - \eta_4|^2) \exp[\mu^2(\eta_1^* z_1 + \eta_2^* z_2 + \eta_3 z_3^* + \eta_4 z_4^* + \eta_3^* \eta_1 + \eta_4^* \eta_2)/2], \end{aligned} \quad (\text{A5})$$

where  $w_A$  is a combinatoric factor equal to 8. We now replace the two coupling functions by their FT’s and then explicitly evaluate the fourfold Gaussian integrals over  $(\eta_i, \eta_i^*)$ . The resulting integrals may then be expressed in the form

$$\begin{aligned} \epsilon C_{4,A}^a &= 4 \left( \frac{\mu^2}{2\pi^2} \right) \exp \left[ \frac{\mu^2(z_1 z_3^* + z_2 z_4^*)}{2} \right] \int \frac{dK dK^*}{2\pi} \exp \left[ -\frac{KK^*}{\mu^2} - \frac{iK^*(z_1 - z_2)}{2} - \frac{iK(z_3^* - z_4^*)}{2} \right] 2\pi \int \frac{dP_1 dP_1^*}{2\pi} \\ &\quad \times \int \frac{dP_2 dP_2^*}{2\pi} \tilde{g}(P_1, P_1^*) \tilde{g}(P_2, P_2^*) \delta(K - P_1 - P_2) \delta(K^* - P_1^* - P_2^*) \exp[(|K|^2 - |P_1|^2 - |P_2|^2 - P_1 P_2^*)/2\mu^2]. \end{aligned} \quad (\text{A6})$$

On comparing the above expression with that for the bare function (A4), we see that the function  $\tilde{g}(K, K^*)$  is renormalized from diagram A by an amount  $\delta\tilde{g}_A$  given by

$$\begin{aligned} \epsilon \delta\tilde{g}_A &= -4\pi \int \frac{dP_1 dP_1^*}{2\pi} \int \frac{dP_2 dP_2^*}{2\pi} \tilde{g}(P_1, P_1^*) \tilde{g}(P_2, P_2^*) \delta(K - P_1 - P_2) \delta(K^* - P_1^* - P_2^*) \exp[(|K|^2 - |P_1|^2 - |P_2|^2 \\ &\quad - P_1 P_2^*)/2\mu^2]. \end{aligned} \quad (\text{A7})$$

In terms of vector notation  $(k_x, k_y)$  this contribution may be written as

$$\epsilon \delta \tilde{g}_A = -2 \int \frac{d^2 p}{2\pi} \tilde{g}(\mathbf{p}) \tilde{g}(\mathbf{k}-\mathbf{p}) \exp[-\mathbf{p} \cdot (\mathbf{p}-\mathbf{k})/\mu^2] \times \cos[(\mathbf{p} \times \mathbf{k})/\mu^2], \quad (\text{A8})$$

where  $\mathbf{p} \times \mathbf{k} \equiv p_x k_y - p_y k_x$ .

In a precisely analogous fashion one may calculate the contributions from diagrams B, C, and D, resulting in the following expressions:

$$\epsilon \delta \tilde{g}_B = -2 \int \frac{d^2 p}{2\pi} \tilde{g}(\mathbf{p}) \tilde{g}(\mathbf{k}-\mathbf{p}) \exp[-\mathbf{p} \cdot (\mathbf{p}-\mathbf{k})/\mu^2], \quad (\text{A9})$$

$$\epsilon \delta \tilde{g}_C = -N \mu^2 \tilde{g}(\mathbf{k})^2 \exp(-k^2/2\mu^2) \quad (\text{A10})$$

and

$$\epsilon \delta \tilde{g}_D = -4 \tilde{g}(\mathbf{k}) \int \frac{d^2 p}{2\pi} \tilde{g}(\mathbf{p}) \exp(-p^2/2\mu^2) \cos[(\mathbf{p} \times \mathbf{k})/\mu^2]. \quad (\text{A11})$$

Given these one-loop renormalizations of the coupling function, we then have the  $\beta$  functional

$$\beta[\tilde{g}] = -\epsilon \tilde{g} + [\delta \tilde{g}_A + \delta \tilde{g}_B + \delta \tilde{g}_C + \delta \tilde{g}_D] + O(\tilde{g}^3). \quad (\text{A12})$$

Interpreting the  $\beta$ -functional as a FRG flow (in terms of a scaling variable  $b=e^l$ ) we may write a differential flow equation of the form  $\partial_l \tilde{g} = -\beta[\tilde{g}]$ . Finally, we define a more convenient coupling function via

$$\tilde{f}(\mathbf{k}) = 2\mu^2 \tilde{g}(\mathbf{k}) \exp[-k^2/2\mu^2] \quad (\text{A13})$$

and then rescale all momenta with respect to  $\mu$ . This completes the derivation of the flow equation (16) given in the main body of the text.

**APPENDIX B**

In this appendix we illustrate the diagrams which contribute to one loop to the renormalization of the four-point correlation function, in the presence of disorder. There will be no explicit calculation in this appendix as the calculations may be easily reconstructed using the examples given in the previous appendix. In the presence of disorder, the labeling of diagrams becomes a little more complicated as we now have replica indices. Referring the reader to the form of the free energy functional in the main text [Eq. (19)], we see that

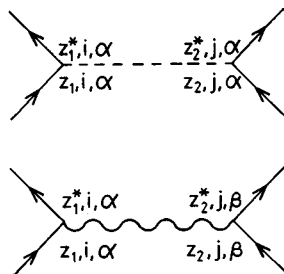


FIG. 7. The two bare vertices in the disorder calculation.

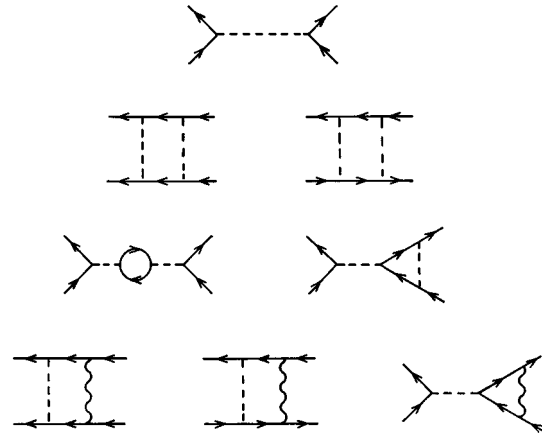


FIG. 8. The bare and one-loop diagrams required for the renormalization of the coupling function  $\tilde{f}$ .

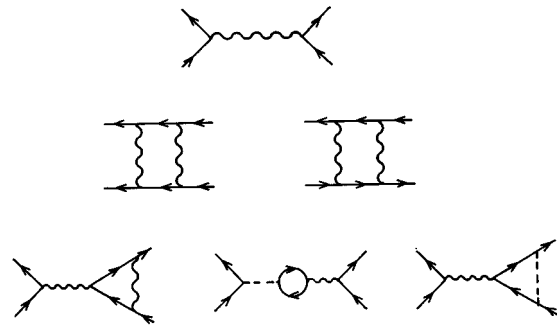


FIG. 9. The bare and one-loop diagrams required for the renormalization of the coupling function  $\tilde{D}$ .

we have two bare vertices which are illustrated in Fig. 7.

As before, we use these vertices to construct the four-point correlation function. Actually, we now require two different correlation functions in order to renormalize the two bare vertices. These correlation functions differ in that one has four identical replica labels ( $\alpha\alpha\alpha\alpha$ ) and will be used to find the renormalization of the coupling function  $\tilde{f}$ , while the other has two pairs of replica labels ( $\alpha\alpha\beta\beta$ ) and will be used to find the renormalization of  $\tilde{D}$ . As before we have two symmetry channels related to the external plane labeling of the diagrams.

In Figs. 8 and 9 we show the bare and one-loop contributions to these four-point correlation functions. Note there are no ‘‘free-loop’’ contributions from the disorder vertex due to the replica limit  $M \rightarrow 0$  (where  $M$  is the number of replicas.)

Following the details of Appendix A, one may finally arrive at the coupled flow equations given in the main text, in Eq. (21).

**APPENDIX C**

In this final appendix we illustrate the diagrams contributing at one loop to the two-point correlation function. By considering these contributions we derive the relation between the fixed point value of the coupling functions, and the shift of the correlation exponent  $\nu$  from its bare value of 2.

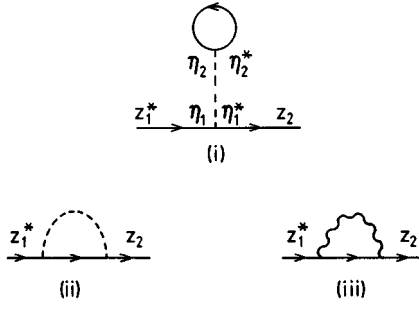


FIG. 10. The three one-loop contributions to the two-point correlation function. We have indicated the internal plane labels in the first diagram to allow comparison with Eq. (C1).

The two-point correlation function at the bare level is simply given by the propagator  $\sigma(\mathbf{q}_\perp; z_1^*, z_2)$ . The one-loop corrections are illustrated in Fig. 10. Note that there is no tadpole contribution from the disorder vertex (because of the replica limit). We shall explicitly evaluate the first diagram, and simply quote the results for the remaining two.

In the limit of the external transverse momentum going to zero, we have for diagram (i) (after performing the usual internal momentum integral)

$$\begin{aligned}
 & -\frac{N}{\tau_0^2} \left( \frac{\mu^2}{2\pi} \right)^3 (-1) \frac{\tau_0^{1-\epsilon/2}}{\epsilon} \int d\eta_1 d\eta_1^* d\eta_2 d\eta_2^* \\
 & \quad \times g(|\eta_1 - \eta_2|^2) \exp[\mu^2(|\eta_1|^2 + |\eta_2|^2)/2] \\
 & \quad \times \exp[\mu^2(|\eta_2|^2 + z_1^* \eta_1 + z_2 \eta_1^*)/2], \quad (C1)
 \end{aligned}$$

where we have added a zero subscript to  $\tau$  to emphasize that it is to be renormalized by these one-loop contributions.

Again, we replace the coupling function by its FT and perform the internal Gaussian integrals. In this way, one obtains for diagram (i)

$$\frac{N}{\tau_0} \left( \frac{\mu^2}{2\pi} \right)^2 \frac{\tau_0^{-\epsilon/2}}{\epsilon} 2\pi \tilde{g}(\mathbf{0}) \exp(\mu^2 z_1^* z_2 / 2). \quad (C2)$$

Comparing this expression to the bare propagator, we see that the inverse mass  $1/\tau_0$  is renormalized by diagram (i) by an amount  $(N/\epsilon\tau_0)\mu^2\tilde{g}(\mathbf{0})$ .

One may show that the analogous contributions from diagrams (ii) and (iii) are given by

$$\frac{2}{\epsilon\tau_0} \int \frac{d^2k}{2\pi} \tilde{g}(\mathbf{k}) \exp(-k^2/2\mu^2)$$

and

$$\frac{-2}{\epsilon\tau_0} \int \frac{d^2k}{2\pi} \tilde{\Delta}(\mathbf{k}) \exp(-k^2/2\mu^2)$$

respectively.

In terms of the functions  $\tilde{f}$  and  $\tilde{D}$  we finally have

$$\begin{aligned}
 \frac{1}{\tau_R} &= \frac{1}{\tau_0} + \frac{1}{\epsilon\tau_0} \left( N\tilde{f}(\mathbf{0}) + \int \frac{d^2k}{2\pi} \tilde{f}(\mathbf{k}) - \int \frac{d^2k}{2\pi} \tilde{D}(\mathbf{k}) \right) \\
 & \quad + O(\tilde{f}^2, \tilde{f}\tilde{D}, \tilde{D}^2). \quad (C3)
 \end{aligned}$$

Following the usual line of argument, this relation may be reexpressed in terms of the shift to the correlation length exponent, as given in the main text in Eq. (22).

\* Address as of 1st January 1996: Department of Physics, University of Manchester, Manchester, M13 9PL, UK.

<sup>1</sup> A.A. Abrikosov, Zh. Eksp. Teor. Fiz. **32**, 1442 (1957) [Sov. Phys. JETP **5**, 1174 (1957)].

<sup>2</sup> E. Brézin, D.R. Nelson, and A. Thiaville, Phys. Rev. B **31**, 7124 (1985).

<sup>3</sup> A.N. Berker, Physica A **194**, 72 (1993).

<sup>4</sup> B.I. Halperin, T.C. Lubensky and S-K. Ma, Phys. Rev. Lett. **32**, 292 (1974).

<sup>5</sup> D. Boyanovsky and J.L. Cardy, Phys. Rev. B **25**, 7058 (1982).

<sup>6</sup> M.A. Moore and T.J. Newman, Phys. Rev. Lett. **75**, 533 (1995).

<sup>7</sup> L. Radzihovsky, Phys. Rev. Lett. **74**, 4722 (1995).

<sup>8</sup> I. Affleck and E. Brézin, Nucl. Phys. **B257**, 451 (1985).

<sup>9</sup> A.L. Fetter and P.C. Hohenberg, in *Superconductivity*, edited by R.D. Parks (Dekker, New York, 1969), Vol. 2.

<sup>10</sup> Z. Tesanovic and A.V. Andreev, Phys. Rev. B **49**, 4064 (1994).

<sup>11</sup> T.C. Lubensky, Phys. Rev. B **11**, 3573 (1975).

<sup>12</sup> D.J. Amit, *Field Theory, the Renormalization Group and Critical*

*Phenomena*, 2nd ed. (McGraw-Hill, New York, 1988).

<sup>13</sup> In Ref. [6] this expression has the wrong sign in the final term.

<sup>14</sup> W.H. Press *et al.*, *Numerical Recipes in C*, 2nd ed. (Cambridge University Press, Cambridge, England, 1992).

<sup>15</sup> D.R. Nelson and B.I. Halperin, Phys. Rev. B **19**, 2457 (1979).

<sup>16</sup> J. Yeo and M.A. Moore (unpublished).

<sup>17</sup> S-K. Ma, *Modern Theory of Critical Phenomena* (Benjamin, New York, 1976).

<sup>18</sup> A.I. Larkin, Sov. Phys. JETP **31**, 784 (1970).

<sup>19</sup> M.A. Moore, Phys. Rev. B **45**, 7336 (1992).

<sup>20</sup> E. Zeldov *et al.*, Nature **375**, 373 (1995).

<sup>21</sup> H. Safar, P.L. Gammel, D.A. Huse, D.J. Bishop, J.P. Rice and D.M. Ginsberg, Phys. Rev. Lett. **69**, 824 (1992).

<sup>22</sup> W.K. Kwok, S. Fleshler, U. Welp, V.M. Vinokur, J. Downey, G.W. Crabtree and M.M. Miller, Phys. Rev. Lett. **69**, 3370 (1992).

<sup>23</sup> J.A. Fendrich *et al.*, Phys. Rev. Lett. **74**, 1210 (1995).

<sup>24</sup> H. Rieger (unpublished).